Figure S1. Evaluating the activity of the screening cell lines. A) 0.2ng of siTat or siGFP control were transfected to the Rev-RRE reporter cell line. After 48 hours, luciferase assays were performed as previously described. This procedure effectively knocked down reporter activity while the mock transfected and siGFP control had only a modest effect on reporter output. Using this method we were able to identify two RRE IIB-Rev cell lines with z' values of 0.69 and 0.75 that were used for the small molecule library screen. B) We also tested the cell lines using the 3,6 diaminoacridine as a control compound that inhibits expression of the reporter.

A.

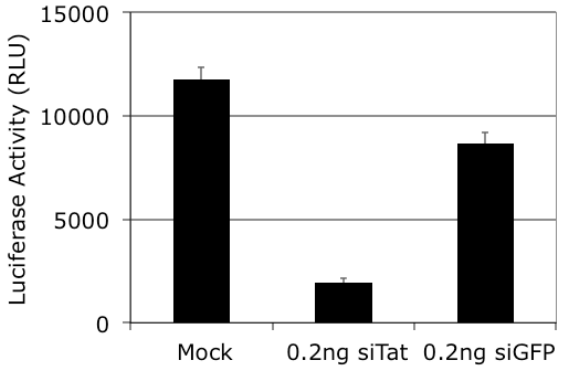

B.

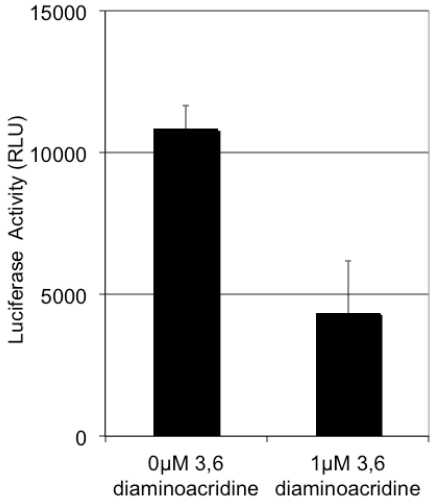

Figure S2. Testing conditions and reproducibility of the screening assay. Compounds were tested in duplicate and luciferase assays were performed. In the graph below the red and blue symbols represent independent duplicate samples. In most cases, the activity levels of the duplicate sample have a difference of less than 10%. In cases in which the variation was greater than 10%, most conferred activation of the luciferase activity, rather than inhibition, and these were not analyzed further. In cases where the duplicates were ambiguous, samples were retested. Most commonly, those compounds were moderately toxic leading to greater variation.

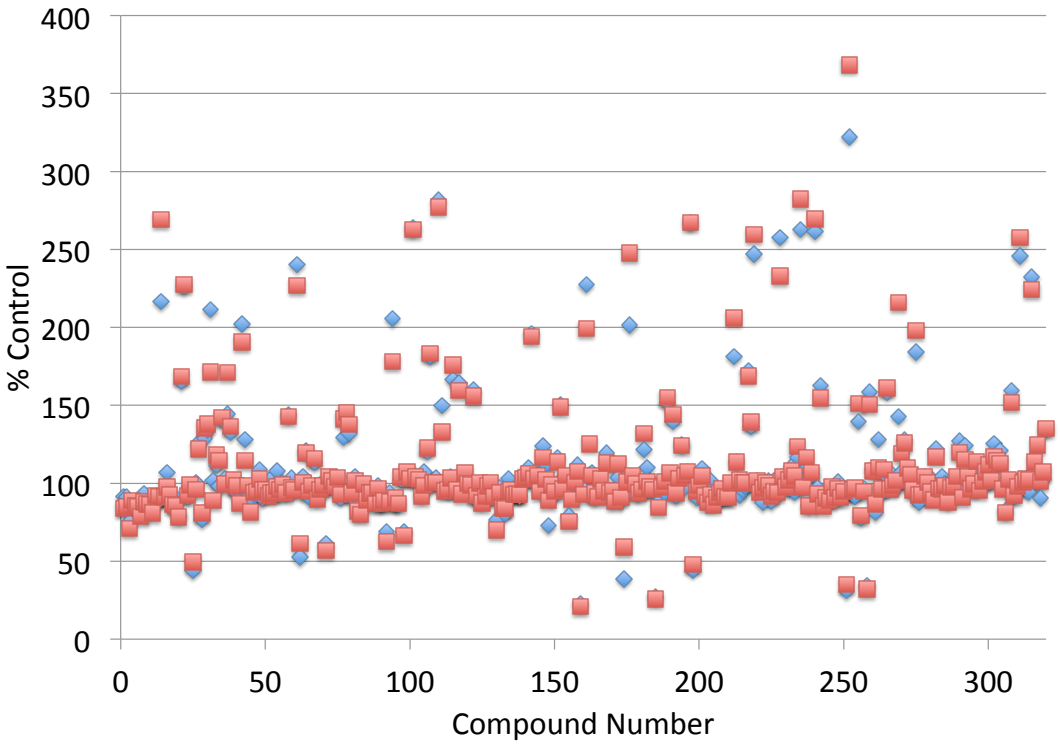

Figure S3. Screening Hits. The compounds in Figure S3 are the hits from the library screen. These compounds conferred greater than 50% inhibition in the screening assay although we did not obtain detailed follow up SAR for the benzopyran or thiophene classes.

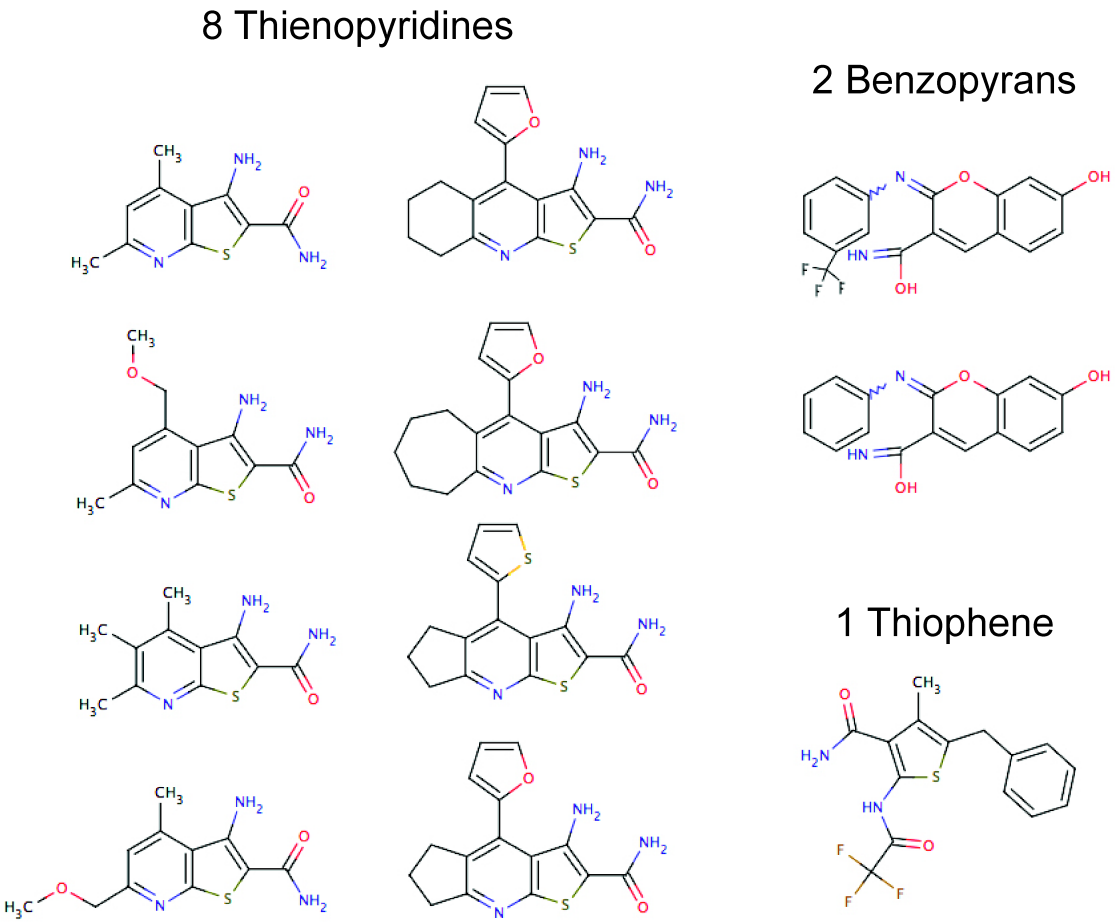

Figure S4. Electrophoretic mobility shift assay (EMSA) reveals inhibition of the Rev-RRE IIB interaction. Titration experiments with RevPeptide and ^{32}P labeled RRE IIB RNA were performed in order to determine conditions in which approximately 50% of the RNA was shifted to a higher mobility as shown in the DMSO lane. Small molecule compounds were incubated in the binding reactions at 100 uM followed by EMSA. The two small molecule control inhibitors 3,6 diaminoacridine and Neomycin B both abolished the shift of the complex suggesting that these compounds disrupt the RNA-protein interaction. Neomycin B treatment consistently results in a shift upwards of the RNA. The two thiophene compounds 1259 and 1267 also inhibited the formation of the shifted complex suggesting that these compounds disrupt the RNA-protein interaction.

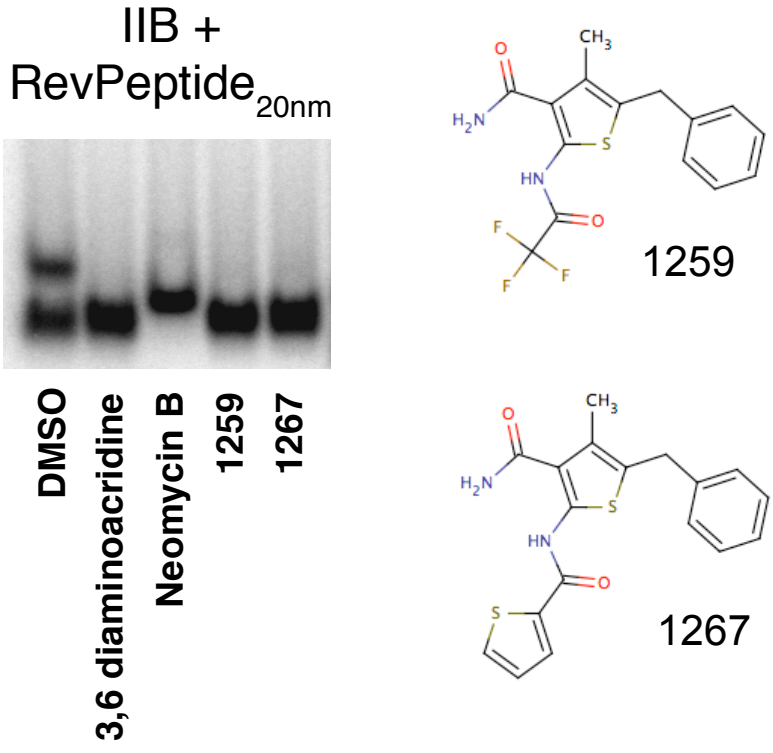

Table S1. Activity of thienopyridine analogs in the U1 latency assay, Tat-hybrid assay, - and MTT toxicity.

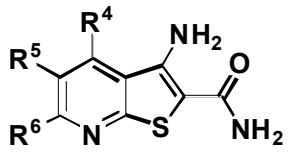

compound	R^4	R^5	R^6	U1 IC_{50} (μM)	Tat-hybrid (%Inhibition)	MTT TC_{50} (μM)
1	Me	Et	Me	0.4	65	>38
2	H	H	Me	2.11	14	>75
3	H	H	*n*-Bu	2.03	0	58.4
4	NMe_2	H	H	<0.28	57	>75
5	CH_2OMe	H	Me	<0.52	63	>75
6	CF_3	H	Me	<0.24	67	>75
7	H	Me	Me	1.06	48	37
8	H	$-CH_2CH_2CH_2-$		2.19	0	>75
9	H	$-CH_2CH_2CH_2CH_2-$		1.94	0	>75
10	H	Me	4-FPh	6.19	8	>75
11	Me	CH_2COPh	Me	0.75	52	>75
12	-NHPh	H	H	<0.24	0	53
13	H	H	pyridyl	23.4	0	>75
14	CF_3	H	Bn	2.37	10	>75
15	4-FPh	H	thiophene	8.84	38	17.4
16	tolyl	H	Ph	0.75	60	22.6
17	4-MeOPh	H	4-MeOPh	1.28	51	38.3
18	4-MeOPh	H	Ph	1.41	51	53.9
19	$-CH_2CH_2CH_2CH_2-$		morpholine	7.13	35	>75

Table S2. Data points and standard deviations for Figure 5.

concentration	**1a**	**2b**	**4e**	**1a stdev**	**2b stdev**	**4d stdev**
1	1.1467	1.5444	1.2524	0.1246	0.3053	0.1577
3.16	1.1400	1.2768	0.6510	0.0411	0.2014	0.1228
10	1.1270	1.0411	0.4718	0.1770	0.1920	0.0704
31.6	1.0482	0.8280	0.2041	0.1075	0.1336	0.0398
100	1.0328	0.4076	0.0926	0.0978	0.0919	0.0114
316	0.8368	0.1144	0.0494	0.0550	0.0533	0.0133
1000	0.5891	0.0332	0.0289	0.0756	0.0059	0.0026
3160	0.2425	0.0061	0.0102	0.0322	0.0106	0.0020

Table S3. Data points and standard deviations for Figure 9.

	day 4	day 6	day 8	day 11
1000nM 2b Average	163.494133	38.3566333	106.99	849.242767
316nM 2b Average	204.4446	89.3033667	3167.51623	12585.9121
100nM 2b Average	199.3502	163.492967	1518.14897	11754.1413
31.6nM 2b Average	188.423167	720.114967	6283.59807	26297.5072
10nM 2b Average	104.504467	537.489633	5866.9493	25967.0032
3.16nM 2b Average	221.809433	1192.81333	8992.60563	34532.432
DmSO Average	302.860683	1201.76435	8349.96183	31162.5508
1000nM 2b Stdev	23.59891	4.13620916	33.8632124	916.415784
316nM 2b Stdev	18.1375439	62.6337768	4858.14671	12828.9292
100nM 2b Stdev	6.39458583	56.6260544	411.19795	1027.3798
31.6nM 2b Stdev	122.831693	503.558663	2803.9239	10631.9251
10nM 2b Stdev	109.166695	229.754705	192.291074	2992.5268
3.16nM 2b Stdev	50.4829612	454.263132	1807.99243	6507.2062
DmSO Stdev	81.0236065	546.562496	872.552606	10617.9197

	day 4	day 6	day 8	day 11
1000nM 4e Average	158.0925	49.8917667	65.9066667	121.052767
316nM 4e Average	96.1949	51.5146	99.7212333	3589.95223
100nM 4e Average	90.8807333	62.1335	132.7636	5075.53777
31.6nM 4e Average	86.1408333	130.8166	686.7589	8367.03223
10nM 4e Average	104.513433	235.257467	2250.9272	15675.262
3.16nM 4e Average	54.0278	289.272467	3405.38157	22545.7145
DmSO Average	167.223967	606.567217	7464.18817	42170.3544
1000nM 4e Stdev	21.70954	7.99158315	32.0080294	61.8425235
316nM 4e Stdev	23.8686368	20.0063079	43.4118813	4717.7648
100nM 4e Stdev	48.80698	10.0520444	20.0198932	6504.37409
31.6nM 4e Stdev	79.3755485	34.0111614	422.655136	3035.82801
10nM 4e Stdev	18.349159	80.4493894	1153.57099	2794.8766
3.16nM 4e Stdev	33.0797158	184.641274	1802.69305	5538.31682
DmSO Stdev	75.5779001	229.199322	1169.04521	7846.60415

	day 4	day 6	day 8	day 11
1000nM 4h Average	74.2060333	66.0407	124.133667	837.503167
316nM 4h Average	60.3931667	72.6754333	140.8883	243.7988
100nM 4h Average	102.4887	95.7632	206.240033	555.0323
31.6nM 4h Average	87.173	138.1644	533.7081	7539.2763
10nM 4h Average	178.409067	208.094533	958.878767	9611.80507
3.16nM 4h Average	278.536	350.3822	3151.4999	21771.2486
DmSO Average	416.676933	1251.20628	9995.91372	38923.4121
1000nM 4h Stdev	37.2094099	10.1005284	34.1845396	1016.17793
316nM 4h Stdev	42.2308501	11.7851801	16.8634793	186.031318
100nM 4h Stdev	65.7043251	12.2973106	77.6353892	592.309721
31.6nM 4h Stdev	7.5600187	22.1995829	20.0614822	2770.18754
10nM 4h Stdev	11.5869841	58.99948	198.571377	234.610719
3.16nM 4h Stdev	10.4016262	69.0497725	389.609229	164.016614
DmSO Stdev	223.003543	505.682275	2205.18098	9489.22884

Testing the specificity of the thienopyridine compounds using the Tat-hybrid reporter system.

We tested the activity of Compound **4a** using the Tat-hybrid reporter assays using the HIV TAR reporter and HIV Tat protein (1-72) that activates this reporter, and compared these results to the Rev-RRE reporter demonstrating good specificity for Rev-RRE, as described below.

A 96 well plate was seeded with 10,000 293T cells. We transfected each well with 10 ng of the HIV TAR Luciferase reporter and 5 ng of the HIV Tat 1-72 expression construct or 10 ng of the HIV RRE IIB Luciferase reporter and 5 ng of the HIV Tat (1-48)-Rev 3-70 expression construct, and with 2 ng of a CMV Renilla luciferase control. Compound **4a** was added to a final concentration of 3.16, 10, 31.6, and 100 nM. Each condition was performed in quadruplet. Note, it was necessary to use transient transfection assays rather than stable cell lines in order to compare the two reporter systems, although the level of inhibition conferred by the compounds in the transient assays was lower than in the cell lines. The cells were incubated for 48 hours and dual luciferase assays were performed according to the manufacturers protocol (Promega). Reporter activity was normalized against the Renilla control. The results of this experiment are shown in Figure S5.

Figure S5. Thienopyridine compound **4a** specifically targets the Rev-RRE reporter. The expression of the HIV RRE IIb reporter was significantly inhibited in the presence of 100 nM Compound **4a** while the expression of the HIV TAR reporter was not similarly inhibited.

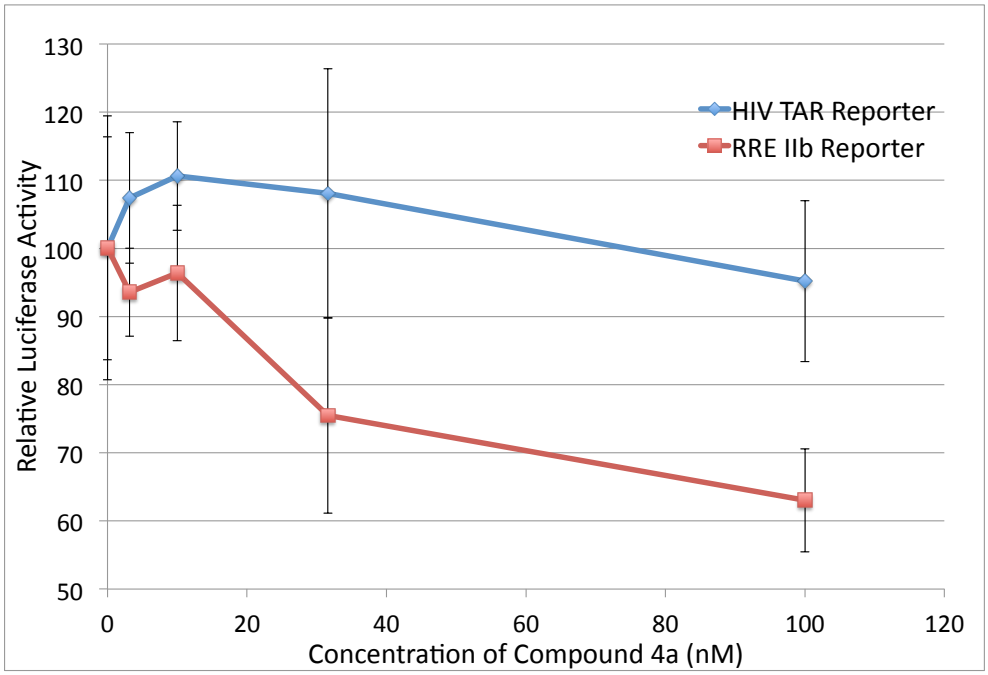

Figure S6. The A7854G mutation in the RRE confers resistance to 62.5 nM **4e**.

Although we were initially concerned that the level of resistance conferred by the resistant-virus (IC_{50} 5.1 nM) was nominal versus the NL4-3 control (IC_{50} 6.2 nM), repeated analysis has shown that resistance is clear, especially at higher concentrations of compound. For example at 62.5 nM of compound **4e**, viral replication occurs at a 4-fold higher rate than the control (below). Notably, the IC_{90} is significantly higher for the A7854G mutant (IC_{90} 218.5 nM) versus the control (IC_{90} 25.9 nM). This result suggests that the target of the thienopyridine compounds is the RRE.